JCARME
ISSN: 2228-7922
Journal of Computational and Applied Research in Mechanical Engineering
Vol. 7, No. 2, pp. 209-222
jcarme.srttu.edu

Three-dimensional chemically reacting radiative MHD flow of nanofluid over a bidirectional stretching surface

C. Siva Krishnama Raju, N. Sandeep* and G. Kumaran

Department of Mathematics, Vellore Institute of Technology, Vellore-632014, Tamil Nadu, India

Article info:

Received: 06/04/2016
Accepted: 23/08/2017
Online: 09/01/2018

Keywords:
MHD,
Sisko ferrofluid,
Non-uniform heat source/sink,
Nonlinear thermal radiation,
Chemical reaction.

Abstract

This study deals with the three-dimensional flow of a chemically reacting magnetohydrodynamic Sisko fluid over a bidirectional stretching surface filled with the ferrous nanoparticles in the presence of non-uniform heat source/sink, nonlinear thermal radiation, and suction/injection. After applying the self-suitable similarity transforms, the nonlinear ordinary differential equations are solved numerically using Runge-Kutta and Newton's methods. Results present the effects of various non-dimensional governing parameters on velocity, temperature and concentration profiles. Also, the friction factor coefficients along with the local Nusselt and Sherwood numbers are computed and discussed. Similarity solutions for suction and injection cases are presented. A good agreement in the present results with the existed literature under some special limited cases is found. It is found that heat and mass transfer performance of Sisko ferrofluid is significantly high in injection case when compared with the suction case. Increasing values of the stretching parameter enhance the heat and mass transfer rate.

1. Introduction

The convective flows over a stretching surface with heat and mass transfer plays an important role in manufacturing industries genuine equipment. So, in the past few decades, the researchers are tremendously interested in the boundary layer flows, which involves non-Newtonian fluid flow over a stretching sheet It has various applications in the field of aerospace, medical, manufacturing of fibers, aerodynamics, biofluids, and marine engineering [1]. An unsteady MHD dusty fluid flow over a stretching surface was discussed by Gireesha et al. [2]. Olajuwon and Oahimire [3] analyzed the MHD and chemical reaction effects on micropolar fluid flow over a rotating frame with thermal diffusion effect. Heat transfer analysis of MHD coupled flow over a permeable oscillating plate in the presence of radiation was investigated by Chauhan and Agarwal [4]. Makine et al. [5] illustrated an unsteady convection flow over a permeable flat plate in the presence of chemical reaction and radiation. Mixed convection flow of a second-

Corresponding author
email address:nsreddy.dr@gmail.com

grade fluid flow over a stretching sheet was examined by Das [6]. MHD convection flow of micropolar fluid flow over a vertical plate in the presence of Soret and Dufour effect was investigated by Srinivasacharya and Upendar [7].

Boundary layer flow of a nanofluid past a stretching sheet in the presence of convective boundary condition was examined by Makinde and Aziz [8]. Olanrewaju et al. [9] discussed the radiation effects on an unsteady convection flow of a Sisko fluid past a flat plate. The boundary layer flow of an incompressible non-Newtonian fluid flow past a nonlinearly stretching surface was discussed by Khan and Shezad [10]. They found that the skin friction coefficient decreases for higher values of power-law index parameter. An unsteady convective heat transfer analysis of an EG-Nimonic 80a nanofluid flow past an infinite vertical plate in the presence of thermal radiation was investigated by Sandeep at al. [11]. Munir et al. [12] analyzed the heat transfer of a Sisko fluid flow over a bidirectional stretching sheet. An axisymmetric flow of non-Newtonian fluid flow over a stretching surface in the presence of thermal radiation was investigated by Khan and Shazad [13]. They proved that the material parameter has a tendency to enhance the velocity profiles. Khan et al. [14] examined the heat transfer characteristics of a Sisko fluid flow inside an annular pipe. The non-uniform heat source/sink effect on ferrofluid flow over a flat plate in the presence of aligned magnetic field and thermal radiation was studied by Raju et al. [15]. Makinde et al. [16] discussed the MHD stagnation point flow and heat transfer of a nanofluid past a convectively heated stretching/shrinking sheet in the presence of buoyancy effects. Hayat et al. [17] studied the boundary layer flow of an Oldroyd-B fluid and viscoelastic fluid over a stretching surface with convective boundary conditions.

The chemical reaction and radiation effects on two-dimensional stagnation point flow of a viscous fluid past a stretching sheet with suction/injection effects were illustrated by Mohan Krishna et al. [18]. Zhou and Yan [19] studied the heat transfer analysis and MHD effect on a nanofluid flow by using lattice Boltzmann process. An unsteady boundary layer MHD nanofluid flow through a stretching sheet with non-uniform heat source/sink and thermophoretic effects were discussed by Sandeep et al. [20]. Hayat et al. [21] illustrated the MHD flow of a nanofluid past an exponentially permeable stretching surface with convective boundary conditions. An unsteady heat transfer analysis of MHD nanofluid flow over a stretching surface in the presence of non-uniform heat source/sink was examined by Shankar and Yirga [22]. Sandeep et al. [23] presented dual solutions for an unsteady MHD flow of a micropolar fluid past a stretching/shrinking surface in the presence of non-uniform heat source/sink. Magneto-nanofluid flow in a rotating frame past an impulsively started porous flat plate was discussed by Das et al. [24]. Animasaun [25] studied the influence of thermophoresis on the free convection flow of MHD dissipative Casson fluid flow. Mutuku-Njane [26] discussed the MHD flow over a permeable vertical plate with convective boundary conditions. Free convective heat transfer of steady/unsteady flows over a stretching surface was analyzed by the researchers [27-31]. Very recently, the researchers [32-35] illustrated the heat and mass transfer behaviour of magnetohydrodynamic flows by considering stretching surface.

In this study, a three-dimensional flow of chemically reacting magnetohydrodynamic Sisko ferrofluid flow over a bidirectional stretching surface in the presence of non-uniform heat source/sink, nonlinear thermal radiation, and suction/injection is analyzed. After applying the self-suitable similarity transforms the transformed nonlinear ordinary differential equations are solved numerically using Runge-Kutta and Newton's methods. Results present the effects of various non-dimensional governing parameters on velocity, temperature, and concentration profiles. Also, computed and discussed the friction factor coefficients along with the local Nusselt and Sherwood numbers.

2. Mathematical formulation

The continuity and momentum equations for this steady flow of an incompressible Sisko nano and ferro fluids with the velocity field $V=\left[u(x,y,z),v(x,y,z),w(x,y,z)\right]$ are stated as follows:

$$\frac{\partial u}{\partial x}+\frac{\partial v}{\partial y}+\frac{\partial w}{\partial z}=0, \tag{1}$$

$$\rho_{nf}\left(u\frac{\partial u}{\partial x}+v\frac{\partial u}{\partial y}+w\frac{\partial u}{\partial z}\right)=-\frac{\partial p}{\partial x}+a\left(\frac{\partial^2 u}{\partial x^2}+\frac{\partial^2 u}{\partial y^2}+\frac{\partial^2 u}{\partial z^2}\right)$$
$$+b\frac{\partial}{\partial y}\left[\left(\frac{\partial u}{\partial y}+\frac{\partial v}{\partial x}\right)\left|\sqrt{\frac{1}{2}trA_1^2}\right|^{n-1}\right]+2b\frac{\partial}{\partial x}\left[\frac{\partial u}{\partial x}\left|\sqrt{\frac{1}{2}trA_1^2}\right|^{n-1}\right]$$
$$+b\frac{\partial}{\partial z}\left[\left(\frac{\partial u}{\partial z}+\frac{\partial w}{\partial x}\right)\left|\sqrt{\frac{1}{2}trA_1^2}\right|^{n-1}\right]-\sigma_{nf}B_0^{\,2}u, \tag{2}$$

$$\rho_{nf}\left(u\frac{\partial v}{\partial x}+v\frac{\partial v}{\partial y}+w\frac{\partial v}{\partial z}\right)=-\frac{\partial p}{\partial y}+a\left(\frac{\partial^2 v}{\partial x^2}+\frac{\partial^2 v}{\partial y^2}+\frac{\partial^2 v}{\partial z^2}\right)$$
$$+b\frac{\partial}{\partial x}\left[\left(\frac{\partial u}{\partial y}+\frac{\partial v}{\partial x}\right)\left|\sqrt{\frac{1}{2}trA_1^2}\right|^{n-1}\right]+2b\frac{\partial}{\partial y}\left[\frac{\partial v}{\partial y}\left|\sqrt{\frac{1}{2}trA_1^2}\right|^{n-1}\right]$$
$$+b\frac{\partial}{\partial z}\left[\left(\frac{\partial v}{\partial z}+\frac{\partial w}{\partial y}\right)\left|\sqrt{\frac{1}{2}trA_1^2}\right|^{n-1}\right]-\sigma_{nf}B_0^{\,2}v, \tag{3}$$

$$\rho_{nf}\left(u\frac{\partial w}{\partial x}+v\frac{\partial w}{\partial y}+w\frac{\partial w}{\partial z}\right)=-\frac{\partial p}{\partial z}+a\left(\frac{\partial^2 w}{\partial x^2}+\frac{\partial^2 w}{\partial y^2}+\frac{\partial^2 w}{\partial z^2}\right)$$
$$+b\frac{\partial}{\partial x}\left[\left(\frac{\partial u}{\partial z}+\frac{\partial w}{\partial x}\right)\left|\sqrt{\frac{1}{2}trA_1^2}\right|^{n-1}\right]++2b\frac{\partial}{\partial z}\left[\frac{\partial w}{\partial z}\left|\sqrt{\frac{1}{2}trA_1^2}\right|^{n-1}\right]$$
$$+b\frac{\partial}{\partial y}\left[\left(\frac{\partial v}{\partial z}+\frac{\partial w}{\partial y}\right)\left|\sqrt{\frac{1}{2}trA_1^2}\right|^{n-1}\right], \tag{4}$$

where

$$\frac{1}{2}tr\left(A_1^2\right)=2\left(\frac{\partial u}{\partial x}\right)^2+2\left(\frac{\partial v}{\partial y}\right)^2+2\left(\frac{\partial w}{\partial z}\right)^2$$
$$+\left(\frac{\partial u}{\partial y}+\frac{\partial v}{\partial x}\right)^2+\left(\frac{\partial v}{\partial z}+\frac{\partial w}{\partial y}\right)^2+\left(\frac{\partial u}{\partial z}+\frac{\partial w}{\partial x}\right)^2, \tag{5}$$

Defining the dimensionless variables and parameters as:

$$u'=\frac{u}{U},v'=\frac{v}{U},w'=\frac{w}{U},x'=\frac{x}{L},y'=\frac{y}{L},z'=\frac{z}{L},$$
$$p'=\frac{p}{\rho U^2},\xi_1=\frac{(a/\rho)}{LU},\xi_2=\frac{(b/\rho)}{LU}\left(\frac{U}{L}\right)^{n-1}, \tag{6}$$

where L is the characteristic length and U is the characteristic velocity. Here the inertial and viscous forces are of the same order of magnitude within the boundary layer, taking $\frac{a/\rho}{LU}\left(\frac{L}{\partial}\right)^2=O(1)$, $\frac{b/\rho}{L^nU^{2-n}}\left(\frac{L}{\partial}\right)^{n+1}=O(1)$ and under the assumption of large Reynolds numbers, Eqs. (1-4), in terms of dimensionless variables, asymptotically can be stated as:

$$\frac{\partial u'}{\partial x'}+\frac{\partial v'}{\partial y'}+\frac{\partial w'}{\partial z'}=0, \tag{7}$$

$$u'\frac{\partial u'}{\partial x'}+v'\frac{\partial u'}{\partial y'}+w\frac{\partial u'}{\partial z'}=-\frac{\partial p'}{\partial x'}+2\xi_2\frac{\partial}{\partial x'}\left[\frac{\partial u'}{\partial x'}\left|\sqrt{\frac{1}{2}trA_1'^2}\right|^{n-1}\right]$$
$$+\xi_1\left(\frac{\partial^2 u'}{\partial x'^2}+\frac{\partial^2 u'}{\partial y'^2}+\frac{\partial^2 u'}{\partial z'^2}\right)++\xi_2\frac{\partial}{\partial y'}\left[\left(\frac{\partial u'}{\partial y'}+\frac{\partial v'}{\partial x'}\right)\left|\sqrt{\frac{1}{2}trA_1'^2}\right|^{n-1}\right]$$
$$+\xi_2\frac{\partial}{\partial z'}\left[\left(\frac{\partial u'}{\partial z'}+\frac{\partial w'}{\partial x'}\right)\left|\sqrt{\frac{1}{2}trA_1'^2}\right|^{n-1}\right]-\sigma_{nf}B_0^{\,2}u', \tag{8}$$

$$u\frac{\partial v'}{\partial x'}+v'\frac{\partial v'}{\partial y'}+w'\frac{\partial v'}{\partial z'}=-\frac{\partial p'}{\partial x'}+\xi_2\frac{\partial}{\partial x'}\left[\left(\frac{\partial u'}{\partial y'}+\frac{\partial v'}{\partial x'}\right)\left|\sqrt{\frac{1}{2}trA_1'^2}\right|^{n-1}\right]$$
$$+\xi_1\left(\frac{\partial^2 v'}{\partial x'^2}+\frac{\partial^2 v'}{\partial y'^2}+\frac{\partial^2 v'}{\partial z'^2}\right)+2\xi_2\frac{\partial}{\partial y'}\left[\left(\frac{\partial v'}{\partial y'}\right)\left|\sqrt{\frac{1}{2}trA_1'^2}\right|^{n-1}\right]$$
$$+\xi_2\frac{\partial}{\partial z'}\left[\left(\frac{\partial v'}{\partial z'}+\frac{\partial w'}{\partial y'}\right)\left|\sqrt{\frac{1}{2}trA_1'^2}\right|^{n-1}\right]-\sigma_{nf}B_0^{\,2}v', \tag{9}$$

$$u'\frac{\partial w'}{\partial x'}+v'\frac{\partial w'}{\partial y'}+w'\frac{\partial w'}{\partial z'}=-\frac{\partial p'}{\partial x'}+\xi_1\left(\frac{\partial^2 w'}{\partial x'^2}+\frac{\partial^2 w'}{\partial y'^2}+\frac{\partial^2 w}{\partial z'^2}\right)$$
$$+\xi_2\frac{\partial}{\partial x'}\left[\left(\frac{\partial u'}{\partial z'}+\frac{\partial w'}{\partial x'}\right)\left|\sqrt{\frac{1}{2}trA_1'^2}\right|^{n-1}\right]$$
$$+\xi_2\frac{\partial}{\partial y'}\left[\left(\frac{\partial v'}{\partial z'}+\frac{\partial w'}{\partial y'}\right)\left|\sqrt{\frac{1}{2}trA_1'^2}\right|^{n-1}\right]$$
$$+\xi_2\frac{\partial}{\partial z'}\left[\left(\frac{\partial w'}{\partial z'}\right)\left|\sqrt{\frac{1}{2}trA_1'^2}\right|^{n-1}\right], \tag{10}$$

$$\frac{1}{2}tr\left(A_1^2\right)=2\left(\frac{\partial u'}{\partial x'}\right)^2+2\left(\frac{\partial v'}{\partial y'}\right)^2+2\left(\frac{\partial w'}{\partial z'}\right)^2$$
$$+\left(\frac{\partial u'}{\partial y'}+\frac{\partial v'}{\partial x'}\right)^2+\left(\frac{\partial u'}{\partial z'}+\frac{\partial w'}{\partial x'}\right)^2+\left(\frac{\partial v'}{\partial z'}+\frac{\partial w'}{\partial y'}\right)^2, \tag{11}$$

By ignoring the small terms in the dimensionless quantities ξ_1 and ξ_2 with $\delta << 1$, the above equations in dimensional form simplifies as:

$$\frac{\partial u}{\partial x}+\frac{\partial v}{\partial y}+\frac{\partial w}{\partial z}=0, \tag{12}$$

$$\rho_{nf}\left(u\frac{\partial u}{\partial x}+v\frac{\partial u}{\partial y}+w\frac{\partial u}{\partial z}\right)=-\frac{\partial p}{\partial x}+a\frac{\partial^2 u}{\partial z^2}+b\frac{\partial}{\partial z}\left[\left|\frac{\partial u}{\partial z}\right|^{n-1}\frac{\partial u}{\partial z}\right]-\sigma_{nf}B_0^{\,2}u', \tag{13}$$

$$\rho_{nf}\left(u\frac{\partial v}{\partial x}+v\frac{\partial v}{\partial y}+w\frac{\partial v}{\partial z}\right)=-\frac{\partial p}{\partial y}+a\frac{\partial^2 v}{\partial z^2}+b\frac{\partial}{\partial z}\left[\left|\frac{\partial u}{\partial z}\right|^{n-1}\frac{\partial v}{\partial z}\right]-\sigma_{nf}B_0^{\,2}v', \tag{14}$$

2. 1. Governing equations

Consider a steady three-dimensional flow of a Sisko ferrofluid over a stretching sheet in the presence of non-uniform heat source or sink, nonlinear thermal radiation, chemical reaction and suction/injection effects. The Sisko ferrofluid occupies the space $z>0$ and it is in motion by an elastic flat sheet in the plane $z=0$, by keeping at a constant temperature, the sheet is being continuously stretched with linear velocities cx and dy in the x and y directions, respectively (see Fig. 1). The constants c and d are positive real numbers relating to stretching of the sheet. Spherical shaped electrically conducting nanoparticles are taken into an account. The ambient temperature and concentration far away from the sheet is uniform and taken as T_∞, C_∞.

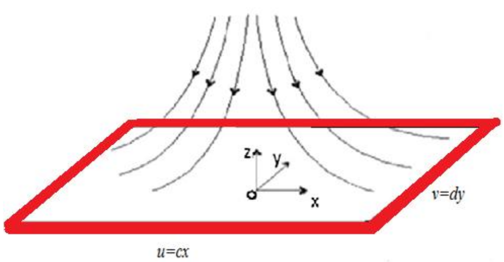

Fig. 1. Physical model of the problem.

The governing steady three-dimensional flow of a Sisko ferrofluid are approximated by the boundary layer theory are:

$$\frac{\partial u}{\partial x}+\frac{\partial v}{\partial y}+\frac{\partial w}{\partial z}=0, \tag{15}$$

$$\rho_{nf}\left(u\frac{\partial u}{\partial x}+v\frac{\partial u}{\partial y}+w\frac{\partial u}{\partial z}\right)=a\frac{\partial^2 u}{\partial z^2}-b\frac{\partial}{\partial z}\left[\left(\frac{\partial u}{\partial z}\right)^{n}\right]-\sigma_{nf}B_0^{\,2}u, \tag{16}$$

$$\rho_{nf}\left(u\frac{\partial v}{\partial x}+v\frac{\partial v}{\partial y}+w\frac{\partial v}{\partial z}\right)=a\frac{\partial^2 v}{\partial z^2}+b\frac{\partial}{\partial z}\left[\left(-\frac{\partial u}{\partial z}\right)^{n-1}\right]\frac{\partial v}{\partial z}-\sigma_{nf}B_0^{\,2}v, \tag{17}$$

$$u\frac{\partial T}{\partial x}+v\frac{\partial T}{\partial y}+w\frac{\partial T}{\partial z}=\frac{k_{nf}}{(\rho c_p)_{nf}}\frac{\partial^2 T}{\partial z^2}+\frac{1}{(\rho c_p)_{nf}}q'''+\frac{1}{(\rho c_p)_{nf}}\frac{\partial q_r}{\partial z}, \tag{18}$$

$$u\frac{\partial C}{\partial x}+v\frac{\partial C}{\partial y}+w\frac{\partial C}{\partial z}=D_B\frac{\partial^2 C}{\partial z^2}-k_l(C-C_\infty), \tag{19}$$

subjected to the following boundary conditions:

$$u=u_w(x)=cx,\ v=v_w(y)=dy,\ w=W,\ T=T_\infty,\ C=C_\infty\ at\ z=0,$$
$$u\to 0, v\to 0, w\to 0, T\to T_\infty, C\to C_\infty\ as\ z\to\infty, \tag{20}$$

Here (u,v,w) are unknown velocity components x,y and z directions, T is the temperature, C is the concentration, W is the suction/injection velocity, D_B is the diffusion coefficient, ρ_{nf} is the density of nanofluid, $(\rho c_p)_{nf}$ is the heat capacitance of nanofluid and k_{nf} is the effective thermal conductivity of nanofluid. These nanofluid constants are given by:

$$(\rho\beta)_{nf} = (1-\phi)(\rho\beta)_f + \phi(\rho\beta)_s,$$
$$(\rho c_p)_{nf} = (1-\phi)(\rho c_p)_f + \phi(\rho c_p)_s,$$
$$\mu_{nf} = \frac{\mu_f}{(1-\phi)^{2.5}}$$
$$\frac{k_{nf}}{k_f} = \frac{(k_s+2k_f)-2\phi(k_f-k_s)}{(k_s+2k_f)+\phi(k_f-k_s)},$$
$$\sigma_{nf} = \sigma_f\left(1+\frac{3(\sigma-1)\phi}{(\sigma+2)-(\sigma-1)\phi}\right), \sigma = \frac{\sigma_s}{\sigma_f},$$
$$\rho_{nf} = (1-\phi)\rho_f + \phi\rho_s, \tag{21}$$

where ϕ is the nano or ferroparticle volume fraction. The subscripts f and s refer to fluid and solid fraction properties, respectively.

The time dependent non-uniform heat source/sink q''' is defined as (Ref. [23]):

$$q''' = \frac{k_f u_w(x)}{x\nu}\left(A^*(T_w-T_\infty)f' + B^*(T-T_\infty)\right), \tag{22}$$

In the above equation, positive values of A^*, B^* correspond to heat generation, negative values correspond to heat absorption, and q_r is the radiative heat flux. Using Roseland approximation, the radiative heat flux is given by (Ref. [3]):

$$q_r = -\frac{4\sigma^*}{3k^*}T^3\frac{\partial T}{\partial z}, \tag{23}$$

where σ^* and k^* are the Stefan-Boltzmann constant and mean absorption coefficients, respectively. Here the energy equation is nonlinear. Now the above equations can be written as:

$$u\frac{\partial T}{\partial x} + v\frac{\partial T}{\partial y} + w\frac{\partial T}{\partial z} = \frac{k_{nf}}{(\rho c_p)_{nf}}\frac{\partial^2 T}{\partial z^2} + \frac{1}{(\rho c_p)_{nf}}q''' + \frac{16\sigma^*}{3k^*(\rho c_p)_{nf}}\frac{\partial}{\partial z}\left(T^3\frac{\partial T}{\partial z}\right), \tag{24}$$

The governing coupled partial differential Eqs. (15-19) are transformed to couple ordinary differential equations by introducing transformation variables:

$$u = cxf'(\eta),\ v = dyg'(\eta),\ w = -c\left(\frac{c^{n-2}}{\rho/b}\right)^{1/n+1}\left(\frac{2n}{n+1}f + \frac{1-n}{1+n}nf' + g\right)x^{(n-1)/(n+1)},$$
$$\theta(\eta) = \frac{T-T_\infty}{T_w-T_\infty} \text{ or } T = T_\infty(1+(\theta_w-1)\theta),$$
$$\eta = z\left(\frac{c^{2-n}}{b/\rho}\right)^{1/n+1}x^{(1-n)/(1+n)}, \psi(\eta) = \frac{C-C_\infty}{C_w-C_\infty}, \tag{25}$$

The momentum and heat transfer equations with the associated boundary conditions reduce to:

$$\frac{\Lambda}{(1-\phi)^{2.5}}f''' + \left(1-\phi+\phi\left(\frac{\rho_s}{\rho_f}\right)\right)\left(\frac{2n}{n+1}ff'' - (f')^2 + gf''\right) - \left[M\left(1+\frac{3(\sigma-1)\phi}{(\sigma+2)-(\sigma-1)\phi}\right)\right]f' + n(-f'')^{n-1}f''' = 0, \tag{26}$$

$$\frac{\Lambda}{(1-\phi)^{2.5}}g''' + \left(1-\phi+\phi\left(\frac{\rho_s}{\rho_f}\right)\right)\left(\frac{2n}{n+1}fg'' - (g')^2 + gg''\right) - \left[M\left(1+\frac{3(\sigma-1)\phi}{(\sigma+2)-(\sigma-1)\phi}\right)\right]f' + (-f'')^{n-1}g''' - (n-1)g''f'''(-f'')^{n-2} = 0, \tag{27}$$

$$\left(\frac{k_{nf}}{k_f} + Ra + Ra(1+(\theta_w-1)\theta)^2\right)\theta'' + 3Ra(\theta_w-1)\theta'^2\left[1+(\theta_w-1)\theta\right]^2 + \left(A^*f' + B^*\theta\right) + \left(1-\phi+\phi\frac{(\rho c_p)_s}{(\rho c_p)_f}\right)\Pr\left(\frac{2n}{n+1}\right)f\theta' + \Pr g\theta' = 0, \tag{28}$$

$$\psi'' + \Pr Le\left(\frac{2n}{n+1}f\psi' + g\psi'\right) - Kr\psi = 0, \tag{29}$$

with the transformed boundary conditions:

$$f(0) = S, g(0) = S,\ f'(0) = 1,\ g'(0) = \lambda,\ \theta(0) = 1, \psi(0) = 1,$$
$$f'(\eta) \to 0,\ f'(\eta) \to 0, \theta(\eta) \to 0,\ \psi(\eta) \to 0 \text{ as } \eta \to \infty, \tag{30}$$

where the prime stand for differentiation with respect to η and λ is the stretching ratio parameter. Further, M is the magnetic field parameter, $\mathrm{Re}_a, \mathrm{Re}_b$ are the local Reynolds number, Λ is the material parameter of Sisko ferrofluid, and $\Pr$ is the generalized Prandtl number, Ra is the radiation parameter, Kr is the chemical reaction parameter, Le is the Lewis number and S is the suction/injection parameter, which are defined as:

$$\mathrm{Re}_a = \frac{\rho x U}{a}, \mathrm{Re}_b = \frac{\rho_f x^n U^{2-n}}{b}, \Lambda = \frac{\mathrm{Re}_b^{\frac{2}{n+1}}}{\mathrm{Re}_a},$$

$$\Pr = \frac{xU R_b^{\frac{-2}{n+1}}}{k_f / (\rho c_p)_f}, Ra = \frac{16\sigma^* T_\infty^{\ 3}}{3kk^*}, Le = \frac{\nu}{D_B}, \tag{31}$$

$$Kr = \frac{k_l}{c}, M = \frac{\sigma_f B_0^{\ 2}}{c\rho},$$

The physical quantities of main interest are the skin-friction coefficients and the local Nusselt number are given by:

$$\frac{1}{2}\mathrm{Re}_b^{\ 1/(n+1)} C_{fx} = (1-\phi)^{-2.5}\left[\Lambda f''(0) - \left(-f''(0)\right)^n\right], \tag{32}$$

$$\frac{1}{2}\mathrm{Re}_b^{\ 1/(n+1)} C_{fy} = (1-\phi)^{-2.5}\frac{v_w}{u_w}\left[\Lambda g''(0) + \left[-f''(0)\right]^{n-1} g''(0)\right] \tag{33}$$

$$\mathrm{Re}_b^{\ -1/n+1} Nu_x = -\theta'(0) \tag{34}$$

$$\mathrm{Re}_b^{\ -1/n+1} Nu_x = -\psi'(0) \tag{35}$$

3. Numerical procedure

The nonlinear ordinary differential Eqs. (26-29) subjected to the boundary conditions (30) are solved numerically using Runge-Kutta and Newton's methods (Mallikarjuna et al. [31]). In this study, the unspecified initial conditions are assumed for unknown variables, and the transformed first order differential equations are integrated numerically as an initial valued problem to a given terminal point. The accuracy of the assumed missing initial condition can be checked by comparing the calculated value of the different variable at the terminal point. These calculations are carried out using Matlab.

4. Results and discussion

The effect of various non-dimensional governing parameters on the velocity, temperature, and concentration profiles along with the friction factor coefficients, local Nusselt, and Sherwood numbers are discussed and presented through graphs and tables. The followings are considered for numerical calculations:

$$\phi = A^* = B^* = 0.1, \lambda = Kr = 0.5,$$
$$Ra = \Lambda = M = 1, \mathrm{Le} = 2, \theta_w = 1.1, n = 3 .$$

Throughout the analysis, these values are kept constant except the values as shown in the corresponding graphs and tables. In this paper, green color indicates suction case and red color indicates the injection case. The thermophysical properties of ferroparticles along with the base fluid are displayed in Table 1.

Figures 2-4 illustrate that the influence of magnetic field parameter on the velocity and temperature profiles of the Sisko ferrofluid. It is evident that an increase in the magnetic field parameter depreciates the velocity profiles and increases the temperature profiles of the flow. Generally, with an increase in the magnetic field parameter the opposite force to flow direction which is called the Lorentz's force is developed. Due to this reason, a fall in the velocity profiles of the flow is seen. It is interesting to mention here that the heat transfer performance is high in the injection case while compared with the suction case.

The influence of ferroparticle volume fraction (ϕ) on the velocity and temperature profiles of the flow for both suction/injection cases are shown in Figs. 5-7. It is noticed that an increasing value of the ferroparticle volume fraction enhances the temperature profiles, whereas it suppresses the velocity profiles of the flow. This may happen due to the improper selection of the nanoparticle volume fraction and low disturbances of the flow.

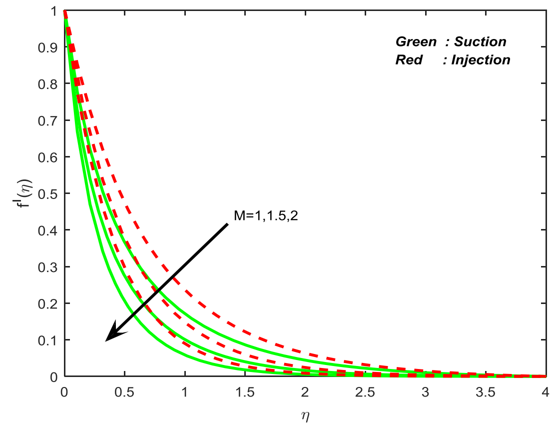

Fig. 2. Velocity field for different values of magnetic field parameter.

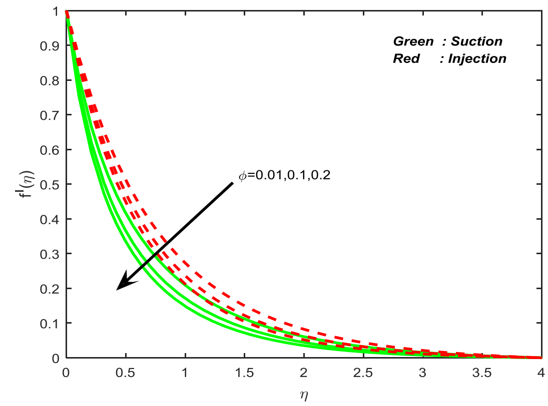

Fig. 5. Velocity field for different values of ferroparticle volume fraction.

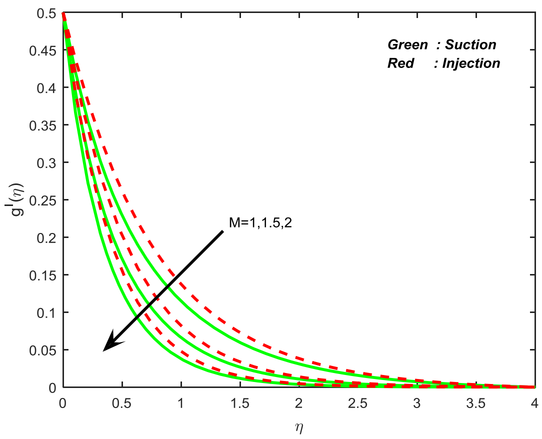

Fig. 3. Velocity field for different values of magnetic field parameter.

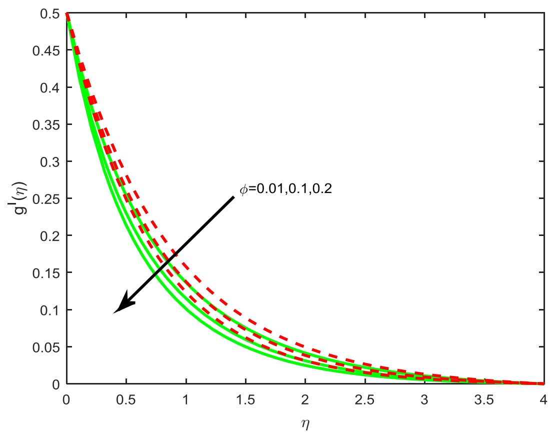

Fig. 6. Velocity field for different values of ferroparticle volume fraction.

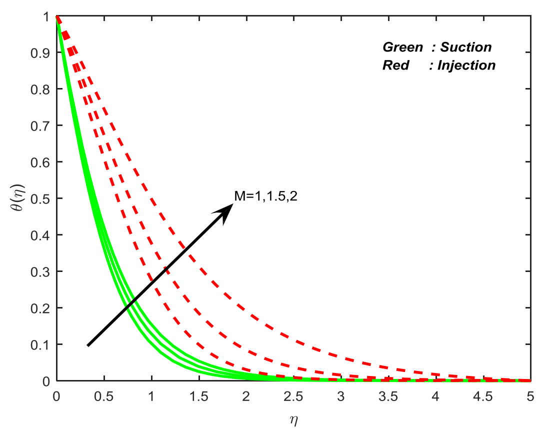

Fig. 4. Temperature field for different values of magnetic field parameter.

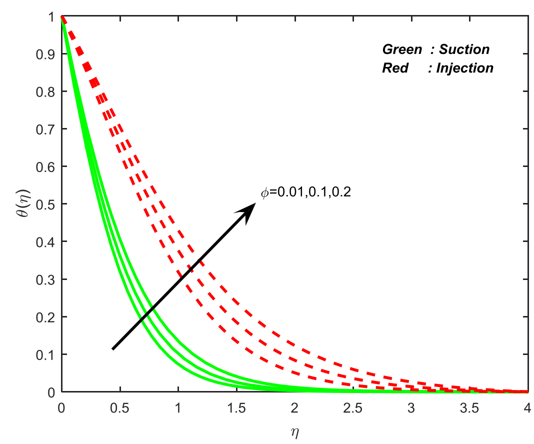

Fig. 7. Temperature field for different values of ferroparticle volume fraction.

The effect of the material parameter (Λ) on the velocity and temperature profiles for both suction and injection cases are displayed in Figs. 8-10. It is clear from these plots that the momentum boundary layer thickness is enhanced with an increase in the material parameter, and temperature profiles show contrary results to it. The similar type of results has been noticed from the Figs. 11-13 with increasing values of the power-law index (n). In the above two cases in the presence of material parameter and power-law index, a rise in the momentum boundary layer thickness of the Sisko ferrofluid is seen. This concludes that Sisko ferrofluid effectively enhances the momentum boundary layer thickness. It is also interesting to mention that the boundary layer thickness is more in presence of injection when compared with suction.

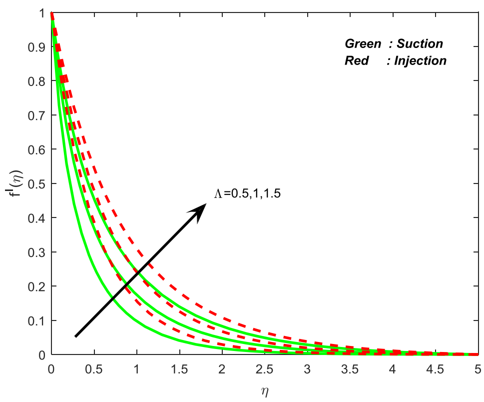

Fig. 8. Velocity field for different values of material parameter.

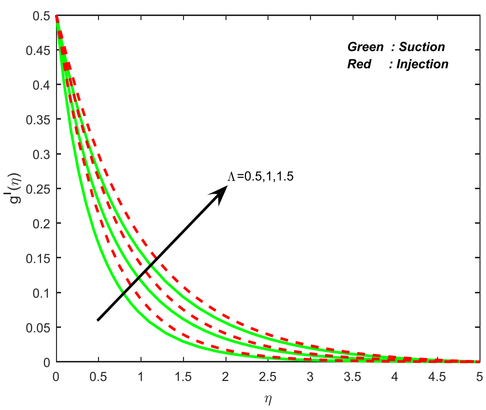

Fig. 9. Velocity field for different values of material parameter.

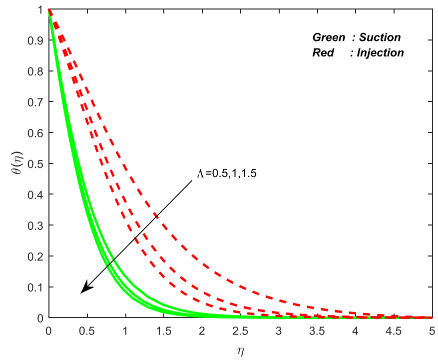

Fig. 10. Temperature field for different values of material parameter.

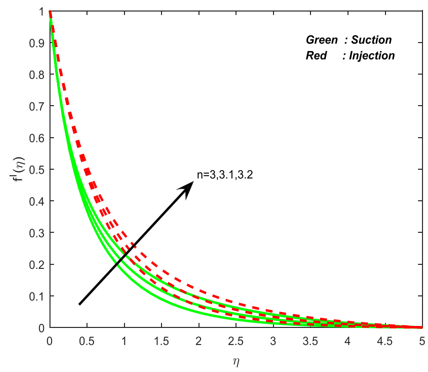

Fig. 11. Velocity field for different values of power law index.

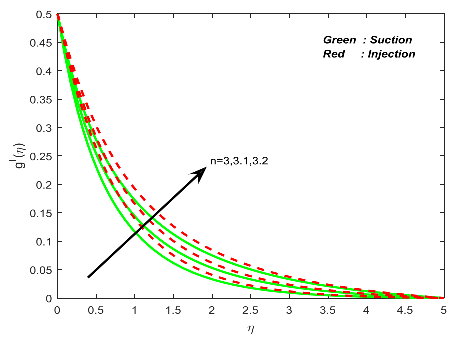

Fig. 12. Velocity field for different values of power law index.

The influence of non-uniform heat source/sink parameter on the temperature profiles of the flow is shown in Fig. 14. It is observed a significant increase in the thermal boundary layer thickness with an increase in the non-uniform heat source/sink parameter. Physically increasing values of the non-uniform heat source/sink parameter releases heat energy to the flow. Due to this reason, an enhancement in the temperature profiles is seen.

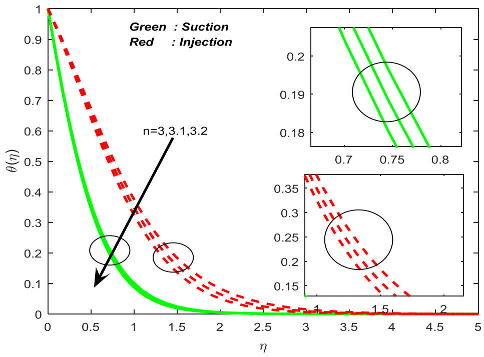

Fig. 13. Temperature field for different values of power law index.

It is prominent to mention here that the positive values of A^* acts like heat generator. The similar type of results is observed with an increase in the nonlinear thermal radiation parameter. This agrees the general physical behavior of the radiation parameter which is displayed in Fig. 15.

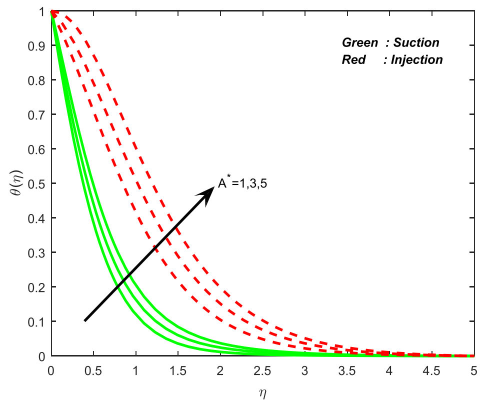

Fig. 14. Temperature field for different values of non-uniform heat source/sink.

Figure 16 depicts the effect of chemical reaction parameter on the concentration profiles of the flow. It is evident that an increasing value of the chemical reaction parameter depreciates the concentration profiles. This is due to an increase in the local interfacial mass transfer in the flow. It is also observed that the influence of chemical reaction is high in the presence of injection.

Figures 17 and 18 illustrate the effect of stretching ratio parameter on velocity and temperature profiles of the flow. It is clear from the plots that increasing values of the stretching ratio parameter enhances the velocity profiles and depreciates the temperature profiles of the flow.

Table 2 represents the comparison of the present results for skin friction coefficients and local Nusselt number with the existed results of Munir et al. [12], Wang [27], and Lui et al. [28] under some special limited cases. An excellent agreement of the present results with the existed results was found. This shows the validity of the present study along with the accuracy of the numerical technique used in this study.

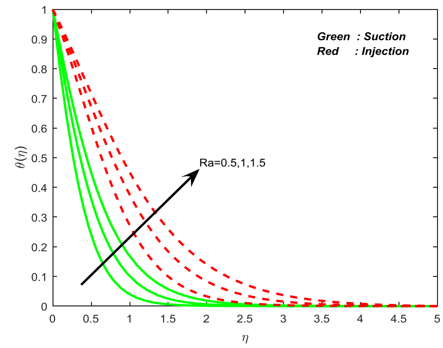

Fig. 15. Temperature field for different values of nonlinear thermal radiation.

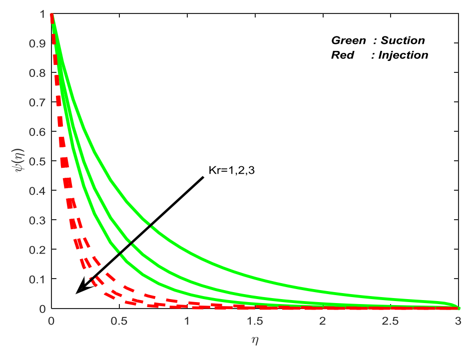

Fig. 16. Concentration field for different values of chemical reaction parameter.

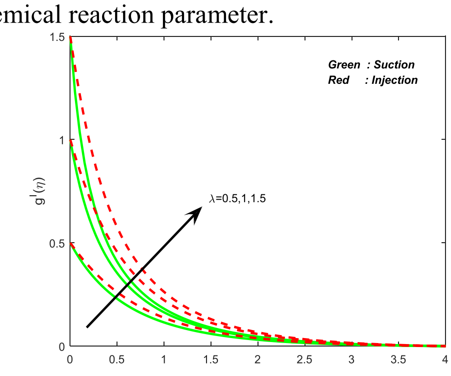

Fig. 17. Velocity field for different values of stretching ratio parameter.

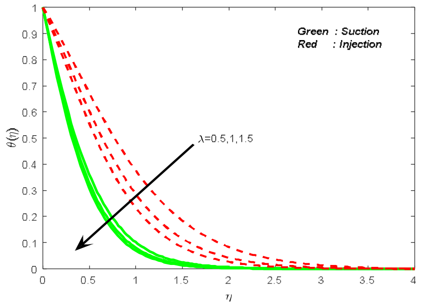

Fig. 18. Temperature field for different values of stretching ratio parameter.

Tables 3 and 4 indicate the effects of various emerging thermophysical parameters on the friction factor coefficients, local Nusselt and Sherwood number for suction and injection cases. It is evident that the friction factor coefficients, heat and mass transfer rates, are enhanced with an increase in the material parameter. The similar types of results are observed with an increase in the power-law index (n). An increase in the ferroparticle volume fraction and magnetic field parameter enhances the local Nusselt number but reduces the friction factors along with the mass transfer rate. Thermal radiation does not influence the friction factor, and mass transfer rate but it helps to reduce the heat transfer rate. Chemical reaction parameter has a tendency to enhance the mass transfer rate.

Table 1. Thermophysical properties of water and ferroparticles.

	$\rho(kg/m^3)$	$c_p(J/kgK)$	$k(W/mK)$	$\sigma(S/m)$
Water	997.1	4179	0.613	5.5×10^{-6}
Fe_3O_4	5180	670	9.7	0.74×10^{6}

Table 2. Comparison of the numerical values of the Skin-friction coefficients and the local Nusselt number, when $M=\phi=\Lambda=A^*=B^*=0, n=1$ for different values of λ.

λ		$-f''(0)$	$-g''(0)$	$\theta'(0)$
0.0	Wang [27]	1	0	-
	Lui et al. [28]	1	0	-
	Munir et al. [12]	1	0	-
	Present Study	1	0.000001	-
0.25	Wang [27]	1.048813	0.194564	-
	Lui et al. [28]	1.048813	0.194564	-0.665933
	Munir et al. [12]	1.048813	0.194564	-0.665939
	Present Study	1.048863	0.194545	-0.670002
0.50	Wang [27]	1.093097	0.465205	-
	Lui et al. [28]	1.093097	0.465206	-0.735334
	Munir et al. [12]	1.093098	0.465207	-0.735336
	Present Study	1.093097	0.466205	-0.735338
0.75	Wang [27]	1.134485	0.794622	-
	Lui et al. [28]	1.134486	0.794619	-0.796472
	Munir et al. [12]	1.134487	0.794619	-0.796472
	Present Study	1.134489	0.794625	-0.796472
1.0	Wang [27]	1.173720	1.173720	-
	Lui et al. [28]	1.173721	1.173721	-
	Munir et al. [12]	1.173721	1.173721	-
	Present Study	1.173720	1.176920	-

Table 3. Numerical values of the Skin-friction coefficients, Nusselt and Sherwood number for suction case.

ϕ	M	Λ	Ra	n	A^*	Kr	λ	$f''(0)$	$g''(0)$	$-\theta'(0)$	$-\psi'(0)$
0.01								-2.128017	-0.719045	1.829309	8.874691
0.1								-2.580015	-0.842045	1.673850	8.839714
0.2								-2.889645	-0.933013	1.517820	8.816191
	1							-2.580015	-0.842045	1.673850	8.839714
	1.5							-3.381193	-1.178863	1.588122	8.770680
	2							-4.187302	-1.518980	1.511145	8.704921
		0.5						-4.023277	-1.236370	1.566608	8.739194
		1						-2.570758	-0.837769	1.675319	8.840659
		1.5						-1.888611	-0.636043	1.739755	8.895611
			0.5					-2.570758	-0.837769	2.274628	8.840659
			1					-2.570758	-0.837769	1.675319	8.840659
			1.5					-2.570758	-0.837769	1.344931	8.840659
				3				-2.570758	-0.837769	1.675319	8.840659
				3.1				-2.643130	-0.756734	1.699003	8.879405
				3.2				-2.698599	-0.668523	1.723445	8.918502
					1			-2.570758	-0.837769	1.565069	8.840659
					3			-2.570758	-0.837769	1.319990	8.840659
					5			-2.570758	-0.837769	1.074804	8.840659
						1		-2.610587	-0.856116	1.669227	2.427537
						2		-2.610587	-0.856116	1.669227	3.377071
						3		-2.610587	-0.856116	1.669227	4.222592
							0.5	-2.580015	-0.842045	1.673850	0.701380
							1	-2.681281	-2.681281	1.793631	0.676530
							1.5	-2.756805	-6.416383	1.873797	0.657656

Table 4. Numerical values of the Skin-friction coefficients, Nusselt and Sherwood number for injection case.

ϕ	M	Λ	Ra	n	A^*	Kr	λ	$f''(0)$	$g''(0)$	$-\theta'(0)$	$-\psi'(0)$
0.0								-1.366335	-0.567689	0.634014	1.551658
0.1								-1.521598	-0.635019	0.576586	1.530831
0.2								-1.628276	-0.686772	0.526492	1.516160
	1							-1.521598	-0.635019	0.576586	1.530831
	1.5							-1.955587	-0.883057	0.455858	1.469728
	2							-2.391369	-1.133237	0.347885	1.412351
		0.5						-1.927866	-0.834551	0.461319	1.475021
		1						-1.517053	-0.631947	0.577916	1.531717
		1.5						-1.251409	-0.510441	0.645616	1.568031
			0.5					-1.517053	-0.631947	0.663976	1.531717
			1					-1.517053	-0.631947	0.577916	1.531717
			1.5					-1.517053	-0.631947	0.512036	1.531716
				3				-1.517053	-0.631947	0.577916	1.531717
				3.1				-1.510755	-0.578088	0.605687	1.537163
				3.2				-1.495857	-0.520053	0.632098	1.543772
					1			-1.517053	-0.631947	0.466124	1.531717
					3			-1.517053	-0.631947	0.217364	1.531715
					5			-1.517053	-0.631947	-0.031850	1.531715
						1		-1.536679	-0.645141	0.576936	7.438455
						2		-1.536679	-0.645141	0.576937	8.711759
						3		-1.536679	-0.645141	0.576937	9.741794
							0.5	-1.521598	-0.635019	0.576587	4.050085
							1	-1.589967	-1.589967	0.718370	3.505575
							1.5	-1.648448	-3.100002	0.824390	3.115003

5. Conclusions

This study presents a numerical solution for the three-dimensional flow of chemically reacting magnetohydrodynamic Sisko ferrofluid flow over a bidirectional stretching surface in the presence of non-uniform heat source/sink, nonlinear thermal radiation, and suction/injection. The conclusions are as follows:

- Suction helps to enhance the momentum and thermal boundary layers of Sisko ferrofluid.
- Magnetic field parameter and volume fraction of ferroparticles have a tendency to enhance the heat transfer rate.
- The positive values of non-uniform heat source/sink parameters acts like heat generators.
- Magnetic field parameter has a tendency to control the flow and reduce the friction factor.
- Suction helps to enhance the concentration boundary layer thickness.
- A rise in the material parameter helps to enhance the heat and mass transfer rate.

References

[1] B. C. Sakiadis, “Boundary layer behavior on continuous solid surfaces”, *American Institute of Chemical Engineering Journal,* Vol. 7, pp. 26-28 (1961).

[2] B. J. Gireesha, J. Manjunatha and C. S. Bagawedi, “Unsteady hydro magnetics boundary layer flow and heat transfer of dusty fluid over a stretching sheet”, *Afrika Matematika*, Vol. 23, pp. 229-241, (2012).

[3] B. I. Olajuwon and J. L. Oahimire, “Effect of thermal radiation and chemical reaction on heat and mass transfer in an MHD micro polar fluid with heat generation”, *Afrika Matematika,* Vol. 25, pp. 911-931, (2014).

[4] D. S. Chauhan and R. Agarwal, “MHD coupled-flow and heat transfer across a porous layer due to an oscillating plate with radiation”, *Afrika Matematika,* Vol. 24, pp. 391-405, (2013).

[5] O. D. Makinde, P. O. Olanrewaju and W. M. Charles, “Unsteady convection with chemical reaction and radiative heat transfer past a flat porous plate moving through a binary mixture, *Afrika Matematika,* Vol. 22, pp. 65-78, (2011).

[6] K. Das, “Effects of thermophoresis and thermal radiation on MHD mixed convective heat and mass transfer flow” *Afrika Matematika,* Vol. 24, pp. 511-524, (2013).

[7] D. Srinivasacharya and M. Upendar, “Soret and Dufour effects on MHD free convection in a micro polar fluid”, *Afrika Matematika,* Vol. 25, pp. 693-705, (2014).

[8] O. D. Makinde and A. Aziz, “Boundary layer flow of a nanofluid past a stretching sheet with convective boundary condition”, *International Journal of Thermal Sciences*, Vol. 50, pp. 1326-1332, (2011).

[9] P. O. Olanrewaju, A. A. Adigun,O. D. Fenwa, A. Oke and A. Funmi, “Unsteady free convective flow of sisko fluid with radiative heat transfer past a flat plate moving through a binary mixture”, *Thermal Energy and power engineering,* Vol. 2, pp. 109-117, (2013).

[10] M. Khan, A. Shazad, “On boundary layer flow of a sisko fluid over a stretching sheet”, *Quaestiones Mathematicae,* Vol. 36, pp. 137-151, (2013).

[11] N. Sandeep, V. Sugunamma and P. Mohan Krishna, “Effects of radiation on an unsteady natural convective flow of a EG-Nimonic 80a nanofluid past an infinite vertical plate”, *Advances in Physics Theories and Applications,* Vol. 23, pp. 36-43, (2013).

[12] A. Munir, A. Shazad and M. Khan, “Convective flow of sisko fluid over a birectional stretching surface”, *Plos One*, Vol. 10, ID: 0130342, (2015).

[13] M. Khan and A. Shahzad, “On axisymmetric flow of sisko fluid over a radially stretching sheet”, *International Journal of Non-linear Mechanics,* Vol. 47, pp. 999-1007, (2012).

[14] M. Khan, S. Munawar and S. Abbasbandy, “Steady flow and heat

transfer of a sisko fluid in annular pipe", *International Journal of Heat and Mass Transfer*, Vol. 53, pp. 1290-1297, (2010).

[15] C. S.K. Raju, N. Sandeep, C. Sulochana and V. Sugunamma, "Effects of aligned magneticfield and radiation on the flow of ferrofluids over a flat plate with non-unifom heat source/sink", *International Journal of Science and Engineering*, Vol. 8, pp. 151-158, (2015).

[16] O. D. Makinde, W. A. Khan and Z.H. Khan, "Buoyancy effects on MHD stagnation point flow and heat transfer of a Nanofluid past a convectively heated stretching/shrinking sheet", *International Journal of Heat and Mass transfer*, Vol. 62, pp. 526-533, (2013).

[17] T. Hayat, B. A. Muhammad, H. A. Hamed and S. A. Muhammad, "Three-dimensional mixed convection flow of viscoelastic fluid with thermal radiation and convective conditions" *Plos One*, Vol. 9, ID: 0090038,(2014).

[18] P. Mohan Krishna, N. Sandeep, and V. Sugunamma, "Effects of Radiation and chemical reaction on MHD convective flow over a permeable stretching surface with suction and heat generation", *Walailak Journal of Science and Technology,* Vol. 12, pp.831-847, (2015).

[19] W. N. Zhou, and Y. Y. Yan, "Numerical investigation of the effects of a magnetic field on nanofluid flow and heat transfer by the lattice Boltzmann method", *Numerical Heat transfer part A: Applications: An International Journal of Computation and Methodology*, Vol. 68, No. 1, pp. 1-16, (2015).

[20] N. Sandeep, C. Sulochana, C. S. K. Raju, and M. Jayachandrababu, " Unsteady boundary layer flow of thermophoretic MHD nanofluid past a stretching sheet with space and time dependent internal heat source/sink, *Applications and Applied Mathematics*, Vol. 10, pp. 312-327, (2015).

[21] T. Hayat, M. Imtiaz, A. Alsaedi and R. Mansoor, "MHD flow of nanofluids over an exponentially stretching sheet in a porous medium with convective boundary conditions", *Chinese Physics B,* Vol. 23, ID: 054701, (2014).

[22] B. Shankar, and Y. Yirga, "Unsteady heat and mass transfer in MHD flow of nanofluids over stretching sheet with a non-uniform heat source/sink", *International Journal of Mathematical, Computational, Statistical, Natural and Physical Engineering,* Vol. 7, No. 12, pp. 1248-1255, (2013).

[23] N. Sandeep and C. Sulochana, "Dual solutions for unsteady mixed flow of MHD micro polar fluid over a stretching/shrinking sheet with non-uniform heat source/sink", *Engineering Science and Technology, an International Journal,* Vol. 18, No. 4, pp. 738-745, (2015).

[24] S. Das, H. K. Mandal, R. N. Jana and O.D. Makinde, "Magneto-nanofluid flow past an impulsively started porous flat plate in a rotating frame", *Journal of Nanofluids,* Vol. 4, pp. 167-175, (2015).

[25] I. L. Animasaun, "Effects of thermophoresis, variable viscosity and thermal conductivity on free convective heat and mass transfer of non-darcian MHD dissipative Casson fluid flow with suction and nth order of chemical reaction", *Journal of the Nigerian Mathematical Society,* Vol. 34, pp. 11-31 (2015).

[26] W. N. Mutuku-Njane, and O.D. Makinde, "MHD nanofluid flow over a permeable vertical plate with convective heating", *Journal of Computational and Theoretical NanoScience,* Vol. 11, pp. 667-675, (2014).

[27] C. Y. Wang, "The three dimensional flow due to a stretching flat surface", *Physics of Fluids,* Vol. 27, pp. 1915-1917, (1984).

[28] I. C. Liu and H. I. Anderson, "Heat transfer over a bidirectional stretching sheet with variable thermal conditions", *International Journal of Heat Mass Transfer*, Vol. 51, pp. 4018-4024, (2008).

[29] W. A. Khan, and I. Pop, "Boundary layer flow of a nanofluid past a stretching sheet", *International Journal of Heat*

and Mass Transfer, Vol. 53, pp. 2477-2483, (2010).

[30] R. S. R. Gorla and I. Sidawi, “Free convection on a vertical stretching surface with suction and blowing”, *Applied Scientific Research,* Vol. 52, pp. 247-257, (1994).

[31] B. Mallikarjuna, A. M. Rashad, A. J. Chamka and S. HariprasadRaju, “Chemical reaction effects on MHD convective heat and mass transfer flow past a rotating vertical cone embedded in a variable porosity regime”, *Afrika Matematica,*Vol. 27, pp. 645-665, (2015).

[32] M. JayachandraBabu and N. Sandeep, “Effect of variable heat source/sink on chemically reacting 3D slip flow caused by a slendering stretching sheet”, *International Journal of Engineering Research in Africa,* Vol. 25, pp. 58-69, (2016).

[33] R. Vijayaragavan,N. Sandeep and S. Karthikeyan, “Cross diffusion effects on chemically reacting radiativeMicropolar fluid flow past a stretching/shrinking sheet”, *Global Journal of Pure and Applied Mathematics,* Vol. 12, No. 3, pp. 370-376, (2016).

[34] J. V. Ramana Reddy, V. Sugunamma, and N. Sandeep, “MHD ferrofluid flow due to bidirectional exponentially stretching surface”, *Global Journal of Pure and Applied Mathematics,* Vol. 12, No. 3, pp. 107-113, (2016).

[35] P. M. Krishna, N. Sandeep, J. V, R. Reddy and V. Sugunamma, “Dual solutions for unsteady flow of Powell-Eyring fluid past an inclined stretching sheet”, *Journal of Naval Architecture and Marine Engineering,* Vol. 13, pp. 89-99, (2016).

How to cite this paper:

C. Siva Krishnama Raju, N. Sandeep and G.Kumaran,“ Three-dimensional chemically reacting radiative MHD flow of nanofluid over a bidirectional stretching surface ”, *Journal of Computational and Applied Research in Mechanical Engineering*, Vol. 7. No. 2, pp. 209-222

DOI: 10.22061/jcarme.2017.1423.1111

URL: http://jcarme.srttu.edu/?_action=showPDF&article=723